Journal of Operation and Automation in Power Engineering
Vol. 6, No. 1, Jun. 2018, Pages: 40-49
http://joape.uma.ac.ir

Characterization of Power Transformer Electromagnetic Forces Affected by Winding Faults

*V. Behjat [1, *], A. Shams [2], V. Tamjidi [1]*

[1]*Department of Electrical Engineering, Azarbaijan Shahid Madani University, Tabriz, Iran*
[2]*Department of Electrical and Computer Engineering, Faculty of Marvdasht, Technical and Vocational University (TVU), Fars, Iran*

Abstract- *Electromagnetic forces in power transformer windings are produced by interaction between the leakage fluxes and current passing them. Since the leakage flux distribution along the windings height is in two axial and radial directions, so the electromagnetic forces have two components, radial and axial. There is a risk that a large electromagnetic force due to the short circuit or inrush currents, can cause the windings to be deform, rupture, and/or displace, if the transformer and winding holders structure is not designed or assembled properly. Also, these mechanical changes can damage insulation between two or more adjacent turns of a winding and so, produce the local inter-turn fault. Occurrence of any fault in windings will change the electromagnetic force distribution in transformers and will cause developing secondary faults. Hence, this contribution is aimed at characterizing the electromagnetic forces behavior in power transformers and determines the changes of force values after occurring winding mechanical and inter-turn. The study keeps at disposal a two-winding, three phase, 8 MVA power transformer, on their windings faults are imposed and investigated through the FEM analysis. The accuracy of the created FEM model is firstly validated using analytical methods for transformer healthy condition, and then the winding shorted turn fault along with the mechanical faults are considered using 3D FEM model. The extracted characteristic signatures attained to different type of winding faults is expected to be useful at the design stage of power transformers.*

Keyword: Power transformer, Electromagnetic forces, Finite element method, Interturn fault, Winding mechanical fault

1. INTRODUCTION

Power transformers as one of the most expensive substation equipment are a major percentage contributor of the initial substation construction expenses. Power transformer failures have many undesirable consequences, including high maintenance costs, reduced network reliability, and increased expected energy not supplied (EENS). During their normal life time, transformer windings are exposed to a variety of electrical, mechanical and thermal stresses. One of the most critical situations is short circuit faults. When a short circuit is occurred, the electromagnetic forces arise in the transformer. These forces can cause damage the windings structure, including bending, destroying or displacement [1]. So, it is very important to investigate the electromagnetic forces distribution of power transformers at the designing stages.

In the last years, various researches have been focused on the investigation of electromagnetic forces distribution and quantity changes on transformer windings due to inrush current or during short circuit conditions [2]. In [3], short circuit analysis for a split-winding transformer using coupled field-circuit is presented. Ref. [4] dealt with three and two dimensional finite element analysis of short circuit force for core type power transformers. In [5], an experimental verification and finite element analysis of short-circuit electromagnetic force has been presented for Dry-type transformer. Different techniques based on the theory of images and finite element method to calculate leakage field and static electromagnetic forces are employed in [6]. Similar research works have been reported in [7-12]. Also, the behavior of three phase transformers with internal faults under sinusoidal and non-sinusoidal operating condition has been investigated in [13]. In addition, Finite element method and discrete wavelet transform have been used for investigate the terminal behavior of the transformers for turn-to-ground and turn-to-turn faults. Ref. [14] has presented a comprehensive force analysis of a 25 MVA power transformer with tap winding under short circuit condition, which concluded that different deformations fault occurrence depend on the tap position. Also, study

Received: 17 June 2016
Revised: 13 Nov. 2016 and 28 July 2017
Accepted: 20 Sep. 2017
∗Corresponding Author:
E-mail: behjat@azaruniv.edu (V. Behjat)
Digital object identifier: 10.22098/joape.2018.2436.1210

on estimation of the transformer windings lifespan in present of electromagnetic force and analysis of force strength on the windings under short circuit current are presented in [15, 16].

Review of highlighted literatures show that the majority of presented research works has been focused on the investigation of electromagnetic forces changes in power transformer windings during short circuit condition or passing inrush current and then, originated winding faults in effect of them. But it also will be so valuable to characterize the electromagnetic forces behavior with the winding electrical and mechanical faults such as winding shorted turn fault as well as winding deformation and/or displacement. So, this paper is concentrated on the FEM modeling of an 8MVA, 20 kV/11 kV power transformers with Delta-Wye connection to perform the study. After verification the performance of developed 3D FEM model using analytical methods for transformer healthy condition, interturn fault and mechanical faults are imposed on the created transformer FEM model. Variations of the flux and electromagnetic forces distribution along the faulted winding are analyzed and investigated which is expected to be useful in understand the changes of electromagnetic forces value and distribution.

2. ELECTROMAGNETIC FORCES AND WINDING MECHANICAL FAULTS

The electromagnetic force is produced by the interaction between the current and magnetic field in a winding. As shown in Fig. 1, the magnetic flux density vector has two radial and axial components, which the radial components are only stronger at the top and bottom ends of the windings. These radial and axial fluxes distribution, lead the resultant electromagnetic force to have two components. Based on the Ampère's force low, if two wires carry current in the same direction, the force between them is attractive and for the opposite direction currents, the force is repulsive. So, the forces between each winding loops are attractive but the force between the two HV and LV windings which are carrying current in the opposite direction is repulsive. Hence, the acting radial forces on the outer winding of the transformer are tensional and trying to rupture the winding conductors, but inner winding of the transformer experiences the radial compressive forces. Also, the axial component of the forces acts on all of

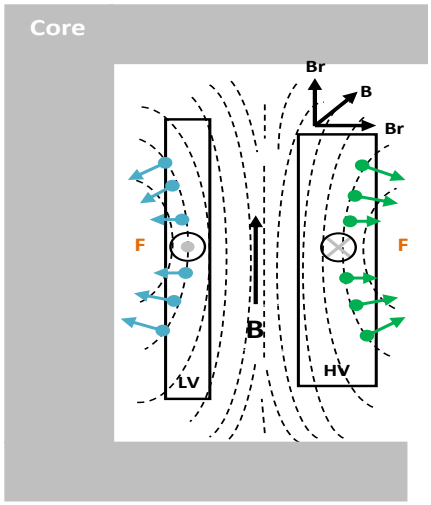

Fig. 1. Electromagnetic forces produced by the interaction between the windings current and leakage flux

2.1. Radial Forces

When a transformer exposes to a short circuit fault, axial leakage flux increases and produces radial forces which act outwards on the outer winding and leads the winding conductors to endure stretch stress [18] and also, cause the inner winding to experience a compressive stress [21], as shown in Fig. 2(a). Different types of the deformations such as free buckling and forced buckling on the inner winding and hoop stress on the outer winding can be occurred due to the radial forces. Fig. 2 illustrates radial forces in a cylindrical winding and various types of radial deformations.

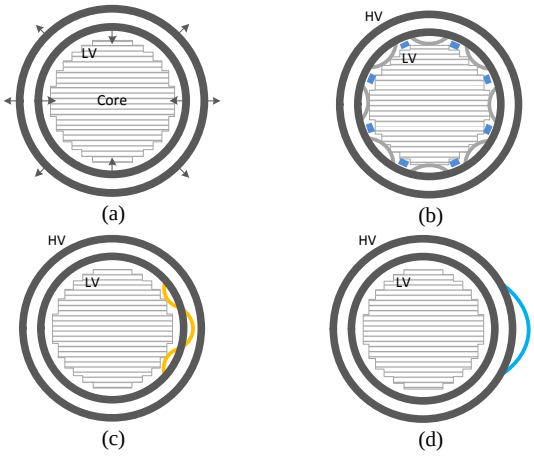

Fig. 2. Electromagnetic radial forces and windings radial deformation, a) Radial forces acting on LV and HV windings, b) HV winding deformation, c) LV winding free buckling, d) LV winding forced buckling

2.2. Axial Forces

The resultant axial forces due to the radial stray flux density, act on all windings and impose an axial displacement or lead the conductors to tilt or bend. The axial forces will be strengthened by Ampere-turn mismatch between the LV and HV windings if the

windings are not situated symmetrically or the HV and LV windings height is not equal. Titling and bending of the conductors between the spacers are one of the most common deformations due to the axial forces [22]. Fig. 3 shows the winding axial forces and the resultant deformations.

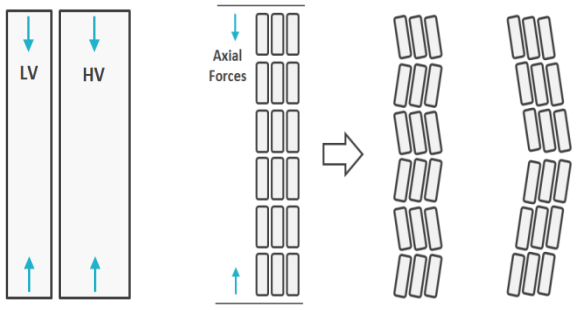

Fig. 3. Electromagnetic axial forces and windings axial deformations, a) Axial forces acting on the windings, b) Winding healthy state, c) Stand-wise tilting, d) Cable-wise tilting

3. WINDING INTER-TURN FAU

During operation of transformer, windings get subjected to a variety of mechanical forces [23], such as: expansion and contraction due to thermal cycling, mechanical vibrations, excessive heating due to overloading and/or inefficient cooling, and forces due to the fault currents. Cumulative effects of these stresses over a span of time result in gradual deterioration of the windings insulation and finally, winding shorted turns fault can be occurred. Fig.4 illustrates an exaggerated presentation of the corresponding geometrical and circuit domain of the transformer coils, assuming that an interturn fault exists on phase "U" of the transformer HV winding.

Winding faults due to such insulation failures has led to the majority of transformer damages over the years. Most winding shorted turns faults initially start as single turn faults due to insulation breakdown that can happen at any time during the operation of the transformers [24, 25].

Incipient stages of an inter-turn insulation failure such as a single turn short circuit fault have negligible impact on the transformer's performance [26]. The changes in the primary and secondary side line currents and voltages are extremely small. Thus, the traditional differential relays [27, 28] which are extensively used for the protection of transformers, cannot detect these faults at an incipient stage to operate the circuit breakers [24, 29].

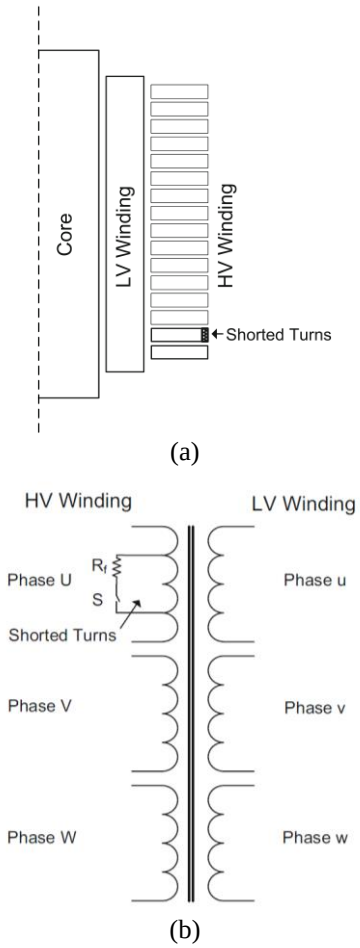

Fig. 4. Geometrical and circuit domain of the transformer coils, assuming that an interturn fault exists on phase "U" of the HV winding

However, during such incipient faults the circulating current induced in the shorted turns can be quite high, as the fault current is opposed only by the resistance and the leakage reactance of the shorted turns of the affected winding, which are very small. This phenomenon leads to a localized thermal overloading in the defective part of the winding; thereby causing hot spots. Over some period of the time, the generated heat causes the fault to increase in size thereby resulting in the shorting of multiple turns. By the time, the fault manifests itself into a severe phase-to-ground fault and the differential relays operate to trip the circuit breakers; a significant part of the transformer winding already gets permanently damaged [26].

Shorted turns will give rise to a large current (circulating current) in the faulted area and also the current of the primary and secondary windings of the transformer will be several times the rated value, which in turn cause to the produced electromagnetic forces be strengthened and so, the winding will be gradually damaged and if continued, it will lead to transformer failure.

4. CALCULATION OF THE ELECTROMAGNETIC FORCES

In this section, two methods are presented for the calculation of the electromagnetic forces: numerical method (FEM) and analytical method.

4.1. Numerical Method

The electromagnetic forces are calculated from the local magnetic flux density in the power transformers. When current flows into the windings of the transformer, the governing equation of the magnetic field is expressed as [5, 18]:

$$\nabla \times \frac{1}{\mu}(\nabla \times A) = J_s - \sigma \frac{\partial A}{\partial t} \qquad (1)$$
$$B = \nabla \times A$$

In Eq. (1), μ is magnetic permeability, A is magnetic vector potential, Js is the current density, σ is the conductivity and B is the flux density. According to Lorentz law, the electromagnetic force becomes [5]:

$$df = idl \times B \qquad (2)$$

The radial and axial components of the magnetic flux density are as follows [30]:

$$B_r = -\sigma \frac{\partial A_\phi}{\partial z}$$
$$B_\phi = 0 \qquad (3)$$
$$B_z = \frac{1}{r}\sigma \frac{\partial A_\phi}{\partial r}$$

Where Br, Bϕ, and Bz are directional components of the flux density in cylindrical coordinate. So, the electromagnetic forces for the radial and axial directions can be computed by using [5]:

$$F = \int_V J_\phi \times \left(B_r \hat{r} + B_z \hat{z} \right) dv = F_r \hat{r} + F_z \hat{z} \qquad (4)$$

$$F_r = B_z \times J_\phi$$
$$F_z = B_r \times J_\phi \qquad (5)$$

As regard to the Eq. (5), the axial leakage flux density B_z, interacts with the current passing from the windings and generates a radial force F_r . As well, interaction between the winding current and radial component of the leakage flux B_r, generates the axial forces F_z.

4.2. Analytical Method

The analytical method for electromagnetic force calculation is completely linear and follows the ideal condition. In normal condition of the transformer, the maximum value of the axial field density (Ba) occurs in the region between the windings and the minimum one is on the internal and external surfaces of the LV and HV windings. So, the radial force Fr (per unit of length) remains practically constant along the length of the windings and can be accurately calculated. The radial component of the force which is produced by the interaction between the instantaneous ampere-turns in each winding (NI) and the leakage field density, can be calculated as Eqs. (6) and (7):

$$B_a = \frac{4\pi(NI)}{10^4}[T] \qquad (6)$$

$$F_r = \frac{2\pi(NI)^2 D_m}{h \times 10^7}[N] \qquad (7)$$

Where N is the number of turns, h is the length of the winding, *Dm* is the mean diameter of the winding and I is the current flowing in the transformer winding.

The analytical calculation of the axial force is not as simple as the radial force calculations. Therefore, there is a well-accepted approach for the above calculation that is the residual Ampere-turns method. According to this method, calculation of axial force can be performed as follow [7]:

$$B_r = \frac{4\pi}{10^4} \times \frac{a(NI)}{2h_{eff}}[T] \qquad (8)$$

$$F_a = \frac{2\pi a(NI)^2}{10^7} \times \frac{\pi D_m}{h_{eff}}[N] \qquad (9)$$

Where a is fractional difference in winding heights and *heff* is the effective length of the path of the radial fluxes that it differs for each arrangement of tapings [30, 32].

5. CASE STYDY

5.1. Finite Element Modeling

In this paper, we deal with an 8MVA, 20 kV/11 kV, Delta-Wye connected power transformer. Fig. 5 illustrates the created 3D FEM model of this transformer. The insulating material and the supporting structure are neglected in this model. For investigate the electromagnetic force distribution on winding height, HV winding is divided into 21 sections. The electromagnetic forces are calculated in each part and then added together to obtain the total amount of forces. Ratings of the considered transformer are presented in Table 1. The FEM model of the studied transformer in healthy state is composed of 761205 volume elements, 81139 surface elements, 20667 line elements and 156777 nodes. The meshes were constructed by using adaptive refinement techniques, so that they are much more refined in the zones of strong variation and high intensity of the magnetic field.

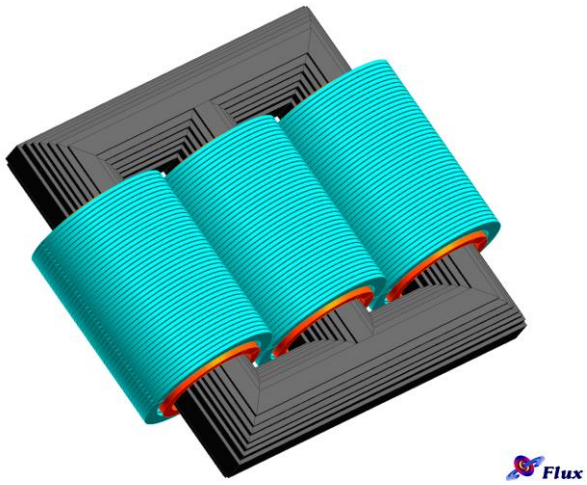

Fig. 5. 3D FEM model of the under study transformer

Table 1. Specifications of the test object

Rated power	8 MVA
Rated frequency	50 Hz
HV rated voltage/current	20 kV/230.9 A
LV rated voltage/current	11 kV/419.9 A
HV winding type	Disk type
LV winding type	Layer type
Connection	Dy11
Turns ratio in normal tap	510/162

5.2. Transformer Normal Condition

When the transformer operates under normal conditions, the electromagnetic forces on the windings are small as the currents and leakage magnetic fluxes are relatively small than the faulty condition. Fig. 6 shows the flux density, radial and axial components of the electromagnetic forces of the transformer in normal condition. As shown in Fig. 6(a), during normal condition, there is very small leakage flux in the space between windings (outside the core), which result in producing low value radial and axial electromagnetic forces. According to Fig. 6(b), the radial force in the central section of the windings has its maximum value, because of the completely axially direction of the flux lines in the middle of the winding. The value of this force is lower at the edges of the winding, because the axial component of the flux lines mostly decreases on winding ends. This force causes compression of the inner winding and opening the outer winding in radial direction. Also, Fig. 6(c) shows that during transformer normal condition, the resultant amount of applied axial forces on the winding is zero. Because the axial forces

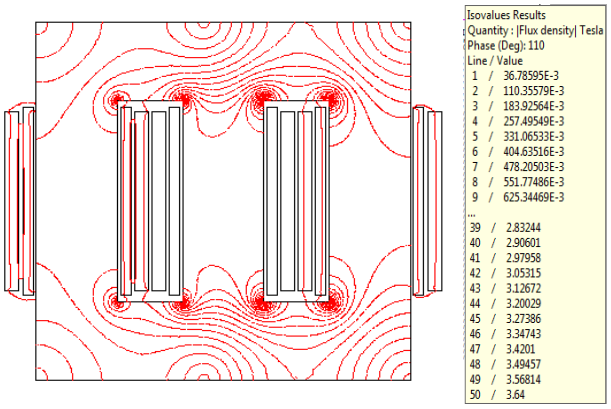

(a)

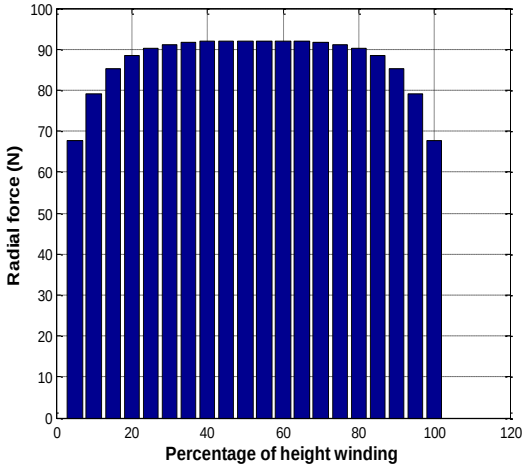

(b)

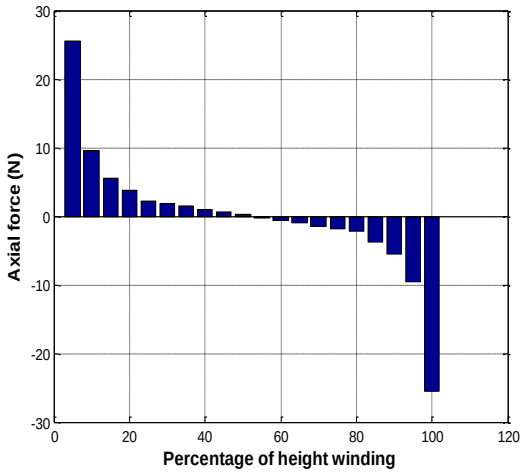

(c)

Fig. 6. Status of transformer under normal condition, a) electromagnetic flux density (Isovalue Results), b) distribution of the radial force of HV winding, c) distribution of the axial force of HV winding

on the upper half of winding is in the negative direction and vice versa, the forces on the lower half of winding is in positive direction. Hence, the net value of the axial forces is zero.

The calculated radial and axial components of the winding electromagnetic force for normal condition of under study transformer are presented in Table 2. The

results derived from the both methods are in close agreement that showing high accuracy of the developed 3D FEM model of the transformer. The difference between results arises from inability of the analytical and FEM 2D method in accurate modeling of both radial and axial fluxes passes in comparison with the FEM 3D modeling.

Table 2. Comparison of the electromagnetic force calculated by FEM and analytical method

	Analytical Method	FEM 2D	FEM 3D
LV Radial Force (N)	1446	1402	1387
LV Axial Force (N)	0.7	0.003	0.3
HV Radial Force (N)	1984	1855	1692
HV Axial Force (N)	0.7	0.003	0.5

5.3. Electromagnetic Force Distribution under Interturn Fault

To investigate the behavior of the electromagnetic forces under winding shorted turns fault, three shorted turn faults including 0.2 percent of HV winding turns in different locations of the winding (25%, 50%, and 75% of winding height (Hw)) are imposed on the 3D FEM model of the transformer.

Figure 7 shows the flux density distribution of the winding under the mentioned shorted turn faults which a larger amount of flux is diverted to the air outside the core. Thus, the leakage fluxes and the resulted radial electromagnetic forces are largely increased at the fault area as it can be seen in Fig. 8. Negative force in the fault location is produced due to the change in the flux direction which causes the winding to be compressed in this region. A significant point is that the value of the radial force in faulty section, directly depends on the fault severity and not the its location.

Axial component of electromagnetic force for shorted turn fault condition are presented in Fig. 9. According to this figure, total axial force is zero in the faulted area; because of the completely radial direction of the flux. The flux in the lateral regions of the shorted turns has changed from axial to radial which causes generate two maximum values of force in different directions. Axial force on the upper half of winding is in the positive direction and on the lower half of winding is in the negative direction that causes the expansion of the winding in axial direction.

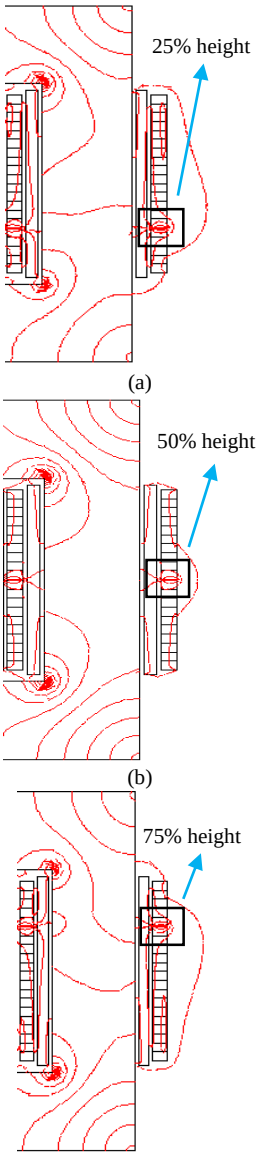

Fig. 7. Flux density distribution (Isovalue Results) in shorted turn fault condition, a) 25% of Hw, b) 50% of Hw, c) 75% of Hw

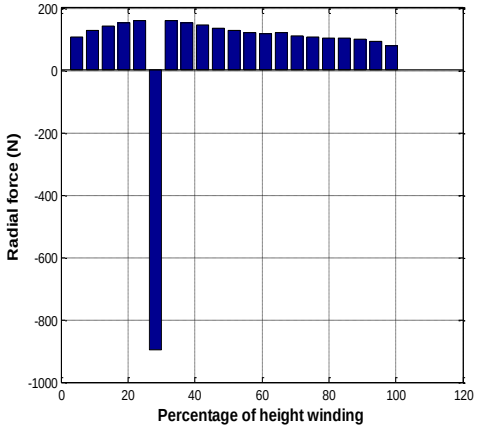

(a)

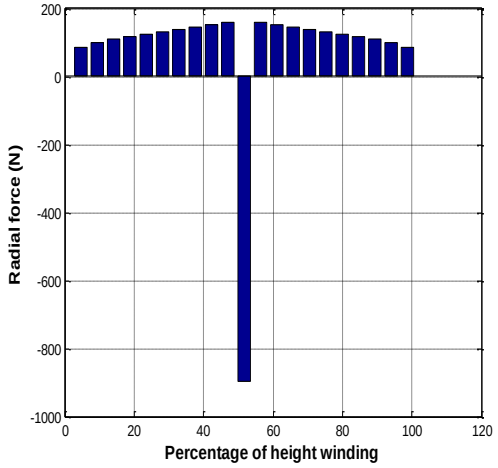

(b)

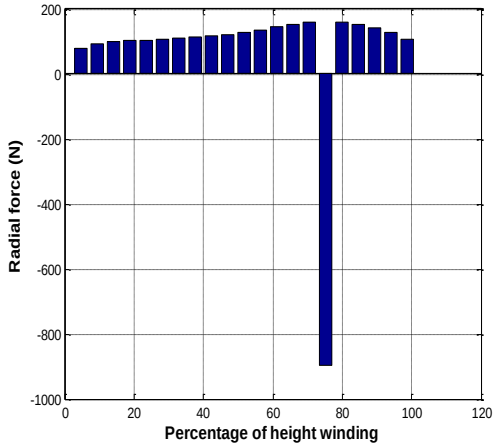

(c)

Fig. 8. Radial force distribution in shorted turn fault condition, a) 25% of Hw, b) 50% of Hw, c) 75% of Hw

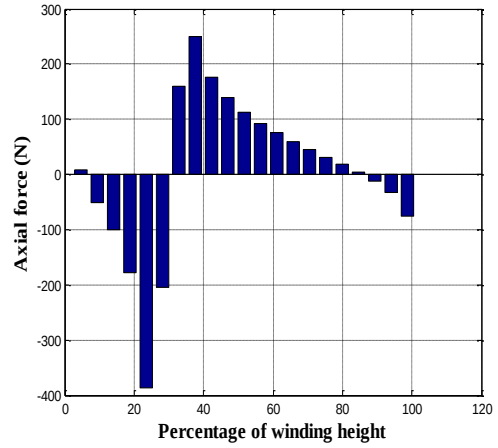

(a)

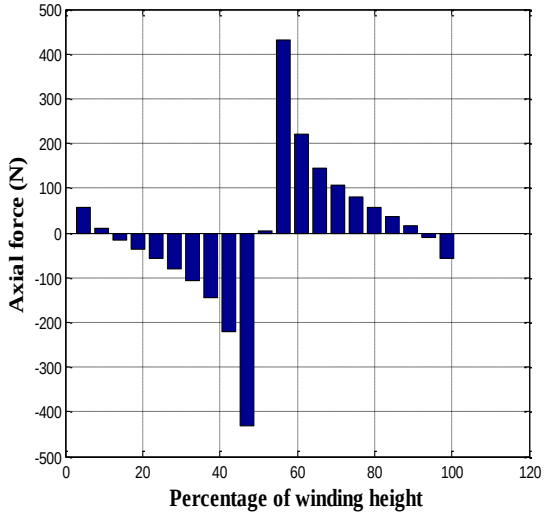

(b)

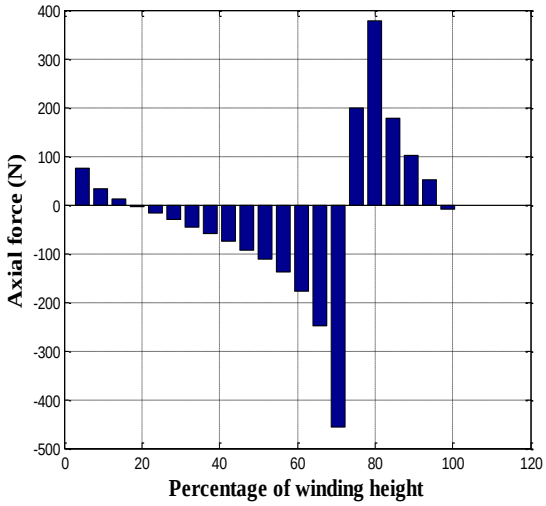

(c)

Fig. 9. Axial force distribution in shorted turn fault condition, a) 25% of Hw, b) 50% of Hw, c) 75% of Hw

5.4. Electromagnetic Force Distribution under winding Mechanical Faults

In this section, the changes of electromagnetic forces under winding mechanical faults are investigated. Fig. 10(a) and (b) shows the axial and radial components of the electromagnetic forces for the HV winding 0 mm (blue), 10 mm (red) and 20 mm (green) upward displacement. The results indicate that when HV winding is shifted upward, peak value of the radial force moves toward to the winding bottom and the total force experiences insensible reductions as winding displacement increases. In the case of axial force, the acting force on each section of the winding increases as winding displacement increases and unlike the radial component, the total axial force experiences drastic

increments which cause the winding to be more displaced over the time. Table 3 shows the radial and axial components of the electromagnetic forces for various displacements.

Table 3. Electromagnetic forces variation under winding axial displacement

Fault Level	Displacement (mm)	Radial Force (N)	Axial Force (N)
1	0	1855	0.0024
2	2	1855	24
3	6	1851	74
4	10	1851	124
5	14	1850	174
6	18	1848	224
7	22	1846	274

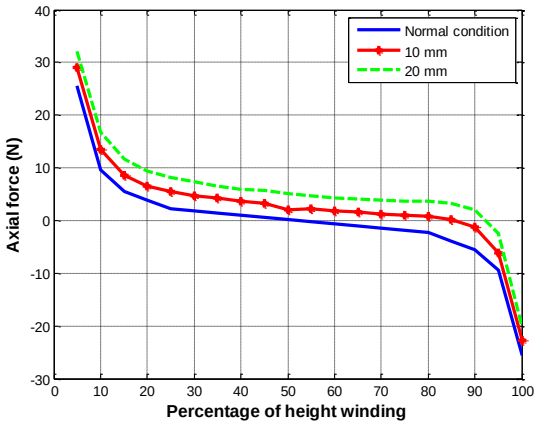

(a)

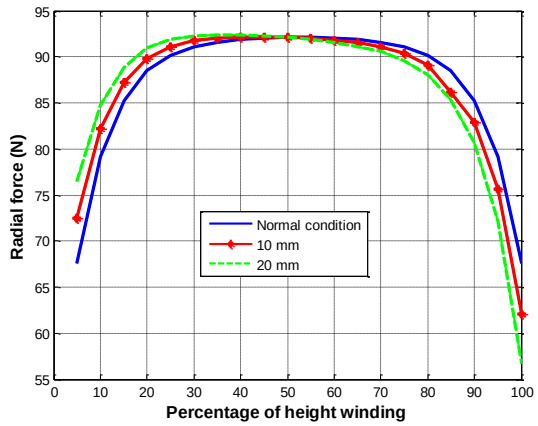

(b)

Fig. 10. Electromagnetic forces distribution under winding axial displacement, a) Axial force and, b) Radial force

According to Fig. 11 (a) and (b), two radial deformations contain free and forced buckling is considered in LV winding. Obtained results from the FEM analysis are presented in Table 4. In regard to the results, with increasing the depth of the winding deformation, the value of the radial electromagnetic forces increases. Fig. 12 shows the radial components of the electromagnetic force for the LV winding (for 10 mm deformation) in normal, free and force buckling condition.

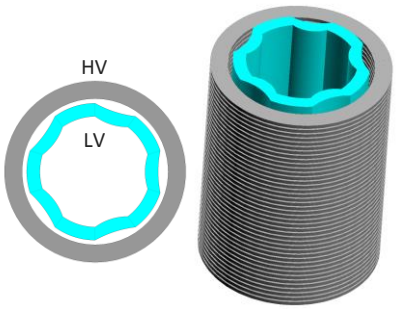

(a)

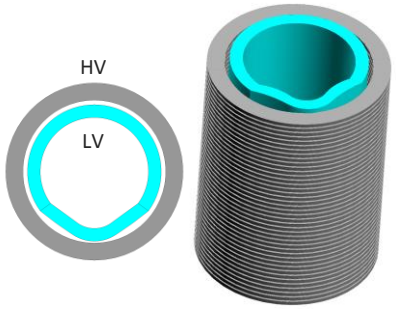

(b)

Fig. 11. LV Winding radial deformation, a) Forced buckling and, b) Free buckling

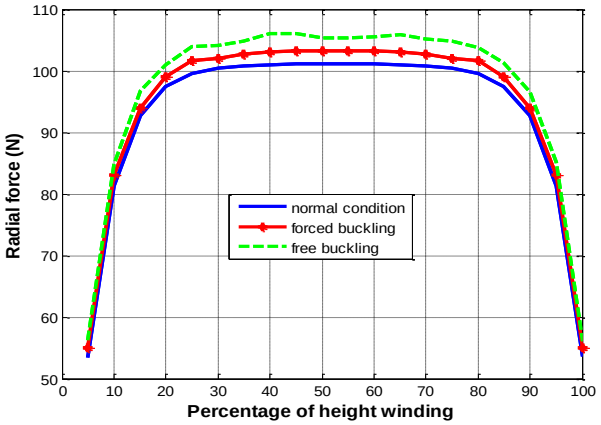

Fig. 12. Radial electromagnetic forces distribution under LV winding buckling

Considering the given results in Table 4, indicate that the radial force increases as the fault level grows. Also the radial force is a little more in the case of the winding free buckling in comparison with the winding forced buckling.

Table 4. Radial electromagnetic force variation under LV winding buckling deformation

Fault Level	Deformation (mm)	Free Buckling (N)	Forced Buckling (N)
1	0	1387	1387
2	2	1420	1410
3	4	1424	1413
4	6	1434	1421
5	8	1450	1433
6	10	1466	1450
7	12	1491	1471

6. CONCLUSIONS

This paper has presented a computational approach using finite element method to obtain electromagnetic forces distribution on the transformer windings under electrical and mechanical fault conditions. Investigations were carried out on an 8 MVA power transformer modeled by FEM and following conclusions can be extracted from results:

In the case of shorted turn fault, the radial electromagnetic forces are largely increased at the fault area, while the axial one is zero. Hence, winding inner supports must be designed and constructed properly to avoiding winding radial deformations.

In the case of the winding deformation, the acting force on the winding sections is increased for both forced and free buckling, but the later imposes a relatively greater force.

In the case of the winding axial displacement, the total radial component of the force experiences negligible reductions as winding displacement increases, while the total axial force experiences drastic increments which is caused that the winding to be more and more displaced over the time.

REFERENCES

[1] Zhang, Z.W., Tang, W.H., Ji, T.Y., Wu, Q.H., "Finite-element modeling for analysis of radial deformations within transformer windings," *IEEE Trans. Power Deliv.*, vol. 25, no. 5, pp. 2297-2305, 2014

[2] A.A. Adly, "Computation of inrush current forces on transformer windings," *IEEE Trans. Magn.,* vol. 37, no. 4, pp. 2855-2857, 2001.

[3] G. B. Kumbhar and S.V. Kulkarni, "Analysis of short-circuit performance of split-winding transformer using coupled field-circuit approach," *IEEE Trans. Power Deliv.,* vol. 22, no. 2, pp. 936-943, 2007.

[4] J. Faiz, B.M. Ebrahimi, and T. Noori, "Three-and two-dimensional finite-element computation of inrush current and short-circuit electromagnetic forces on windings of a three-phase core-type power transformer," *IEEE Trans. Magn.,* vol. 44, no. 5, pp. 590-597, 2008.

[5] H.M. Ahn, J.Y. lee, J.K. Kim, and Y.H. Oh, "Finite-element analysis of short-circuit electromagnetic force in power transformer," *IEEE Trans. Ind. Appl.,* vol. 47, no. 3, pp. 1267-1272, 2011.

[6] A.G. Kladas, M.P. Papadopoulos, and J.A. Tegopoulos, "Leakage flux and force calculation on power transformer windings under short-circuit: 2D and 3D models based on the theory of images and the finite element method compared to measurements," *IEEE Trans. Magn.,* vol. 30, no. 5, pp. 3487-3490, 1994.

[7] A.C. De Azevedo, I. Rezende, A.C. Delaiba, J.C. De Oliveira, "Investigation of transformer electromagnetic forces caused by external faults using FEM," *In Proc. of the IEEE PES Transm. Distrib. Conf. Exposition: Lat. Am.*, 2006.

[8] Y.Q. Tang, J.Q. Qiao, and ZH. Xu, "Numerical calculation of short circuit electromagnetic forces on the transformer winding," *IEEE Trans. Magn.,* vol. 26, no. 2, pp. 1039-1041, 1990.

[9] T. Renyuan, L. Yan, L. dake, T. Lijian, "Numerical calculation of 3D eddy current field and short circuit electromagnetic force in large transformers," *IEEE Trans. Magn.,* vol. 28, no. 2, pp. 1418-1421, 1992.

[10] S. Jamali, M. Ardebili, and K. Abbaszadeh, "Calculation of short circuit reactance and electromagnetic forces in three phase transformer by finite element method," *Electr. Mach. Syst. In Proc. Of the 8th Int. Conf.,* vol. 3, 2005.

[11] M. Ardebili, K. Abbaszadeh, S. Jamali, H.A. Toliyat, "Winding arrangement effects on electromagnetic forces and short-circuit reactance calculation in power transformers via numerical and analytical methods," *In Proc. of the IEEE 12th Biennial Conf.,* 2006.

[12] M., Zhiqiang and Z. Wang, "The analysis of mechanical strength of HV winding using finite element method. Part I Calculation of electromagnetic forces," *Univ. Power Eng. Conf.,* vol. 1, 2004.

[13] N.Y. Abed and O.A. Mohammed, "Modeling and characterization of transformers internal faults using finite element and discrete wavelet transforms," *IEEE Trans. Magn.,* vol. 43, no. 4, pp. 1425-1428, 2007.

[14] K. Guven and T. Gundogdu, "Effect of the tap winding configurations on the electromagnetic forces acting on the concentric transformer coils,"

In Proc. of the 3rd Int. Conf. Electr. Power Energy Convers. Syst., 2013.

[15] J. F. Araujo, E. G. Costa, F. L. M. Andrade, A. D. Germano, and T. V. Ferreira, "Methodology to Evaluate the Electromechanical Effects of Electromagnetic Forces on Conductive Materials in Transformer Windings Using the Von Mises and Fatigue Criteria," *IEEE Trans. Power Deliv.*, vol. 31, no. 5, pp. 2206-2214, 2016.

[16] D. Geißler; T. Leibfried, "Short-Circuit Strength of Power Transformer Windings-Verification of Tests by a Finite Element Analysis-Based Model*," IEEE Trans. Power Deliv.*, vol. 32, no. 4, pp. 1705-1712, 2017.

[17] N. Hashemnia, A. Abu-Siada and S. Islam, "Improved power transformer winding fault detection using FRA diagnostics – part 1: axial displacement simulation," *IEEE Trans. Dielect. Elect. Insul.*, vol. 22, no. 1, pp. 556-563, 2015.

[18] S.V. Kulkarni and S.A. Khaparde, *Transformer engineering: design and practice*, vol. 25. CRC Press, 2nd ed, 2012.

[19] W. J McNutt, W.M.Johnson, and R.A.Nelson, "Power transformer short-circuit strength-requirements, designer, and demonstration," *IEEE Trans. Power Appl. Syst.*, PAS-89, no. 8, pp. 1955-1969, 1970.

[20] R.M. Del-Vecchio, B. Poulin, and P.T. Feghali, Transformer design principles: with applications to core-form power transformers, FL: CRC Press, US, 2nd ed, 2010.

[21] J.A.S.B. Jayasinghe and Z.D. Wang, "Winding movement in power transformers: a comparison of FRA measurement connection methods," *IEEE Trans. Dielect. Elect. Insul.*, vol. 13, no. 6, pp.1342-1349, 2006.

[22] M. Bagheri, S.N. Mohammad, and T. Blackburn, "Advanced transformer winding deformation diagnosis: moving from off-line to on-line," *IEEE Trans. Dielect. Elect. Insul.,* vol. 19, no. 6, pp. 1860-1870, 2012.

[23] IEEE Guide for Protective Relay Applications to Power Transformers, IEEE C37.91-2000.

[24] L.M.R. Oliveira and A.J. Cardoso, "On-line diagnostics of transformer winding insulation failures, by Park's Vector Approach," *In Proc. of the 9th Int. Electr. Insul. Conf.*, 2001.

[25] K.L. Butler-Purry, M. Bagriyanik, M.J. Mousavi, P. Palmer-Buckle, "Experimental investigation of internal short circuit faults leading to advanced incipient behavior and failure of a distribution transformer," In Proce. *IEEE PES Power Syst. Conf. Expos.*, 2004.

[26] V. Behjat and A. Vahedi, "An experimental approach for investigating low-level interturn winding faults in power transformers," *Spring Electr. Eng.*, vol. 95, no. 2, pp. 135-145, 2013.

[27] B. Ravindranath and M. Chander, *Power syst. Protection. switchgear*, New Age International, 1977.

[28] Y.G. Paithankar, S.R. Bhide, *Fundamentals of Power System Protection*, PHI Learning Pvt. Ltd. 2004.

[29] A. Vahedi and V. Behjat, "Online monitoring of power transformers for detection of internal winding short circuit faults using negative sequence analysis," *Eur. Trans. Electr. Power*, vol. 21, no. 1, pp. 196-211, 2011.

[30] M.R. Feyzi and M. Sabahi, "Finite element analysis of short circuit forces in power transformers with asymmetric conditions," *In Proce. of the IEEE Int. Symp. Ind. Electron.*, pp. 576-581, 2008.

[31] A.C. Franklin, D.P. Franklin, The J&*P* Transformer Book, Butterworth Ltd, London, 1993.

[32] The Short Circuit Performance of Power Transformers, Brochure CIGRE WG 12.19, 2002.